Paper Presented at the XVIII International Conference on High Energy Physics, Tbilisi, U.S.S.R. July 15-21 1976.

BNL-21620

Conf-760719--7

Radiative Decays of K^o_L Mesons*

A.S. Carroll, I-H. Chiang, K.K. Li, L.S. Littenberg,

M.D. Marx, T.F. Kycia, and P.O. Mazur†

Brookhaven National Laboratory, Upton, New York 11973

W.C. Carithers and J-P. de Brion‡

University of Rochester, Rochester, New York 14627

ABSTRACT

In an experiment at the Brookhaven National Laboratory AGS we have studied a number of radiative decays of the K^o_L ($\pi^+\pi^-\gamma$, $e^+e^-\gamma$ and $\mu^+\mu^-\gamma$). The charged particles from these decays were detected in a 5000 wire proportional chamber spectrometer and the gammas were detected in a 194 element lead glass Cerenkov counter array.

Preliminary results, based on ~ 25% of our total data sample, are as follows: The branching ratio $K^o_L \to \pi\pi\gamma(\text{direct})/K^o_L \to \text{all} = 5.5 \pm 1.0 \times 10^{-5}$. One example of the previously unobserved decay $K^o_L \to ee\gamma$ has been found, yielding a branching ratio of $8.3 \pm 8.3 \times 10^{-6}$. No examples of the decays $K^o_L \to \mu\mu\gamma$, $ee\pi^o$, and $\mu\mu\pi^o$ were found, yielding improved upper limits of $K^o_L \to \mu\mu\gamma/K^o_L \to \text{all} < 1.3 \times 10^{-6}$, $K^o_L \to ee\pi^o/K^o_L \to \text{all} < 1.4 \times 10^{-5}$, $K^o_L \to \mu\mu\pi^o/K^o_L \to \text{all} < 2.5 \times 10^{-6}$ with 90% confidence.

---

*Work supported by the Energy Research and Development Administration.
†Present address: Fermi National Accelerator Laboratory, Batavia, Illinois 60510.
‡Present address: CEN-Saclay, 91190 Gif sur Yvette, France.

DISCLAIMER

We present preliminary results of an experiment to measure the rare radiative decays $K^o_L \rightarrow \pi^+\pi^-\gamma$, $e^+e^-\gamma$, and $\mu^+\mu^-\gamma$. The experiment was also sensitive to certain other rare decay modes such as $e^+e^-\pi^o$ and $\mu^+\mu^-\pi^o$.

$K^o_L \rightarrow \pi^+\pi^-\gamma$ is important as a decay which might exhibit CP violation and as a proving ground for various theories of weak radiative decays.[2] The decays $K^o_L \rightarrow e^+e^-\gamma$ and $\mu^+\mu^-\gamma$ have been suggested as sites for possible anomalous effects[3] and structure[4], which would manifest themselves as deviations from the rate and matrix elements which can otherwise be calculated reliably[5] given the measured $K^o_L \rightarrow \gamma\gamma$ rate. $K^o_L \rightarrow e^+e^-\pi^o$ and $\mu^+\mu^-\pi^o$ are important as tests of higher order effects in weak interactions.[6]

The experiment was carried out at the Brookhaven National Laboratory AGS in a neutral beam off the internal G-10 target. Three collimators defined a solid angle of 18 μsr at an angle of 4.7^o to the circulating proton beam. Eight radiation lengths of uranium in the beam directly ahead of the first collimator were used to convert the γ rays. Two sweeping magnets eliminated charged particles in the beam. The beam contained $\sim 10^6$ K^o_L and $\sim 2 \times 10^7$ neutrons/pulse. The K^o_L momentum averaged ~ 6 GeV/c and the useful spectrum extended from 2 to 16 GeV/c.

The experimental arrangement is shown in Figure 1. The neutral beam passed through a veto counter (D) and into a 6m vacuum decay tank. Charged products of the decays were detected in a 3-chamber 5000 wire MWPC spectrometer system which has been described previously.[7] With the magnetic field set to give a transverse momentum kick of 105 MeV/c the system had a mass resolution of $4 MeV/c^2$ for $K^o_L \rightarrow \pi^+\pi^-$ decays. A hydrogen Cerenkov counter (C) at atmospheric pressure with 12 independent optical sectors (C_i) could distinguish electrons from pions at momenta below 8 GeV/c. Muons with momenta greater than 1.5 GeV/c were identified by their penetration of 780 grams/cm^2 of material (mostly heavy concrete).

To be accepted as a muon, a particle had to fire the appropriate scintillator in each of two hodoscopes, one placed after 600 gms, and the other after the full 780 gms. The first hodoscope (μ_H) consisted of eight horizontal counters four on each side of the beam, while the second (μ_V) contained eight vertical counters. Muons were accepted with > 95% probability,[7] whereas a study of kinematically unambiguous $K^o_L \rightarrow \pi^+\pi^-\pi^o$ decays demonstrated that only ~ 4% of pions satisfied these conditions.

Photons were detected in a 194-element lead glass Cerenkov counter array. The array was divided into 2 hodoscopes. The front wall consisted of 32-7.5 x 15.0 x 45.0 cm^3 and 6-7.5 x 15.0 x 22.5 cm^3 counters arranged vertically in 2 rows, each presenting 7.5 cm (2.6r.1.)of lead glass to the beam. The rear wall consisted of an 8 x 20 array of 15.0 x 15.0 x 25 cm^3 counters, each presenting 25 cm (8.5 r.1.) to the beam. A 45 x 45 cm^2 hole was left in the center of the front wall and a 30 x 30 cm^2 hole was left in the center of the rear wall to allow passage of the beam. Analogue information from each counter was gated into a separate ADC channel. Short term calibration of the counter was accomplished by means of an Am 241 doped sodium iodide crystal glued to the front face of each block, while long term calibration was provided by position and momentum analyzed electrons from the copious K_{e3} decays. A 38-element scintillation counter hodoscope (UV) placed between the front and rear walls provided fast timing information on both charged and neutral particles. The lead glass hodoscope achieved an energy resolution of $\frac{\sigma_E}{E} = \frac{6.5\%}{\sqrt{E(\text{GeV})}}$ and a position resolution of $\sigma_x \sim 1.2$ cm for electron and photon showers. Two large lead-liquid scintillator shower counters (γ_{anti}) flanked the aperture of the upstream face of the analyzing magnet. These counters, set in anticoincidence, served to reduce the trigger rate due to $K^o_L \rightarrow \pi^+\pi^-\pi^o$ decays in which only one γ strikes the lead glass array.

The electronic triggering requirements were as follows.

All modes: $(\overline{D})\cdot(\overline{\gamma_{anti}})\cdot$(2 in each spectrometer plane)$\cdot$($\geqslant$ 3 clusters in UV timing counters)

$\cdot$($\geqslant$ 3 clusters in the lead glass rear wall).

$\pi\pi\gamma$: (above)$\cdot(\overline{\mu_H \cdot \mu_V})\cdot\overline{C}$

$ee\gamma$[8]: (above)$\cdot(C_i T_i)\cdot(C_j \cdot T_j)$

$\mu\mu\gamma$: (above)$\cdot(2\mu_H)\cdot(2\mu_V)$

In addition many runs were taken under special triggering conditions, e.g. K_{e3} and $K_{\mu 3}$ runs, runs with the γ_{anti} switched out, etc. For each event data from the MWPC's, ADC's, TDC's, latches, etc. were collected via CAMAC by a PDP-15 computer which performed various monitoring tasks and wrote the events onto magnetic tape. A fraction of the events were transmitted via an on-line link to a PDP-10 computer for reconstruction.

Altogether, approximately 2.7×10^7 events were collected. The present paper is based on an analysis of ~ 25% of the data. The vast majority of these were $K^o_L \rightarrow \pi^+\pi^-\pi^o$ events, where neither γ from the π^o decay struck the γ_{anti}. About 10% of the $K^o_L \rightarrow \pi^+\pi^-\pi^o$ recorded had both γ's detected in the lead glass. These were used as a running normalization for the experiment.

Figure 2 shows the two-γ mass spectrum of a sample of $\pi^+\pi^-\gamma\gamma$ events. A clear π^o peak with a resolution of σ = 8.7 MeV/c^2 is evident. When we plot the 4 body $\pi^+\pi^-\gamma\gamma$ effective mass for events in the π^o peak we get the histogram shown in Figure 3, a virtually background-free K^o mass peak with a resolution of σ = 12 MeV/c^2.

Candidates for all modes considered in this paper were required to meet the following criteria; (1) good decay vertex within a fiducial volume in the vacuum chamber, (2) at least one in-time γ, (3) γ and charged tracks within a fiducial area at the lead glass array, (4) γ and charged track clusters separated in both lead glass and UV timing counters.

The $\pi\pi\gamma$ candidates also had to satisfy; (1) E_γ^{LAB} > .2 GeV/c^2, (2) $PO2^9$ <-.002, (3) .480 < $M(\pi\pi\gamma)$ < .520 GeV/c^2, (4) $(1 - \cos\theta_{\pi\pi\gamma}) < 0.3 \times 10^{-5}$ (where $\theta_{\pi\pi\gamma}$ is the angle between the incoming kaon direction and the 3-momentum of the final state), (5) no C_i fired, and (6) neither charged track satisfied the good μ conditions.

The $ee\gamma$ candidates had to satisfy; (1) appropriate C_i and T_i counters fired, (2) neither charged track satisfied the good μ conditions, (3) each charged track satisfied $.5 < p_{LAB} \leq 8$ GeV/c, (4) for each charged track the ratio (energy deposited in the lead glass)/(momentum as measured in the spectrometer) was between 0.75 and 1.25, (5) PO2 <-.002, (6) .480 < M $(ee\gamma)$ < .520 GeV/c^2, and (7) $(1-\cos\theta_{ee\gamma}) < 0.3 \times 10^{-5}$.

The $ee\pi^o$ candidates had to satisfy $ee\gamma$ conditions (1) - (4) above, and (5) a second γ was present within the lead glass fiducial area, (6) .105 < $M(\gamma\gamma)$ < .165 GeV/c^2, (7) .480 < M $(ee\pi^o)$ < .520 GeV/c^2, and (8) $(1-\cos\theta_{ee\gamma\gamma}) < 0.3 \times 10^{-5}$.

The $\mu\mu\gamma$ candidates had to satisfy: (1) for each track an appropriate μ_V and μ_H fired, (2) for each charged track $1.5 < p_{LAB} < 7$ GeV/c, (3) no C_i fired, (4) for each charged track the lead glass pulse height was in the minimum ionizing range, (6) $.480 < M_{\mu\mu\gamma} < .520$ GeV/c^2, and (7) $(1-\cos\theta_{\mu\mu\gamma}) < 0.3 \times 10^{-5}$.

The $\mu\mu\pi^o$ candidates had to satisfy $\mu\mu\gamma$ conditions (1) - (4) above, and (5) a second γ was present within the lead glass fiducial area, (6) $.105 < M(\gamma\gamma) < .165$ GeV/c^2, (7) $.480 < M(\mu\mu\pi^o) < .520$, GeV/c^2 and (8) $(1-\cos\theta_{\mu\mu\gamma\gamma})$ $< 0.3 \times 10^{-5}$.

The normalization $K^o_L \rightarrow \pi^+\pi^-\pi^o$ candidates had to satisfy; (1) no C_i fired, (2) neither charged track satisfied the good-μ conditions, (3) a second in-time γ was present within the lead glass fiducial area, (4) All 4 clusters in the lead glass and in the UV timing counters were distinct, (5) $.105 < M(\gamma\gamma) < .165$ GeV/c^2, (6) $.460 < M(\pi^+\pi^-\gamma\gamma) < .535$ GeV/c^2, and (7) $(1-\cos\theta_{\pi\pi\gamma\gamma}) < 0.3 \times 10^{-5}$.

The normalization procedure was as follows. The detection efficiency for $K^o_L \rightarrow \pi^+\pi^-\pi^o$ decay under the above conditions was calculated by means of a Monte Carlo program. Then the number of K decays in a given sample, N, was set equal to the observed $K^o_L \rightarrow \pi^+\pi^-\pi^o$/(detection efficiency x BR($K^o_L \rightarrow \pi^+\pi^-\pi^o$)). The $K^o_L \rightarrow \pi^+\pi^-\pi^o$ branching ratio was taken to be 0.1225[10]. Then for each decay mode, the detection efficiency was calculated again via the Monte Carlo program, and the branching ratio was set equal to N^{-1} x (Number of observed events/detection efficiency) for that mode. This method of normalization has the advantage of being unaffected by uncertainties in the incoming K^o beam flux, and of being largely invulnerable to rate effects. Also, particularly in the case of $\pi\pi\gamma$, the normalization events are topologically extremely similar to the decay mode being measured. Counter inefficiencies, etc. tend to cancel in this case. One disadvantage of this method in the $\pi\pi\gamma$, $\mu\mu\gamma$, and $ee\gamma$

cases is that the $K^o_L \to \pi^+\pi^-\pi^o$ events have one more γ than the mode being normalized. This makes the normalization more sensitive to uncertainties in the γ efficiency, and the probability of shower spreading. In order to assess the Monte Carlo program in this respect we took a number of special runs in which the γ anti counters were removed from the trigger. Then the number of $K^o_L \to \pi^+\pi^-\pi^o$ decays in which only 1 γ is detected can be compared with the Monte Carlo prediction, made on the basis of the 2γ sample. These events are almost identical to $\pi\pi\gamma$ events in their sensitivity to γ efficiency, shower spreading, UV counter efficiency, etc. The number of single-γ $K^o_L \to \pi^+\pi^-\pi^o$ events agreed with the prediction to within 20%.

Figure 4 shows the mass spectrum for a sample of $\pi\pi\gamma$ candidates in which all of the cuts except that on $M(\pi\pi\gamma)$ have been imposed. The $K^o_L \to \pi\pi\gamma$ peak is clearly visible. The background peak centered around .440 GeV/c^2 is due mainly to $K^o_L \to \pi^+\pi^-\pi^o$ decays in which one of the charged tracks was scattered or decayed before the last MWPC. It is evident that this background is clearly separable from the $\pi\pi\gamma$ events. Figure 5 shows the distribution in $(1-\cos\theta_{\pi\pi\gamma})\times 10^5$ of a sample of $\pi\pi\gamma$ candidates passing all the other cuts. Again a clear peak with little background is evident. Figure 6 shows the distribution in k^*, the γ c.m. energy of all events passing all $\pi\pi\gamma$ cuts. The spectrum falls rapidly as k^* increases in a manner consistent with inner-bremsstrahlung, and then starts rising again to peak near 100 MeV as would be expected from a CP conserving M1 direct γ emission.[2] In fact, as shown on the figure, this spectrum is well fit[11] by the sum of the distributions given by these two matrix elements when they are inserted into the Monte Carlo program. Unfortunately, the inner bremsstrahlung region ($k^* < 60$ MeV) is partly contaminated by a background due to $K^o_L \to \pi^+\pi^-$ decays in which one pion interacts in material downstream of the MWPC's (particularly in the lead glass front wall), producing an extra shower in the lead glass which is then mistaken for a photon. If the $\pi\pi$ mass also fluctuates to the low side of the K^o_L mass, the phenomenon can yield an event which will pass the $\pi\pi\gamma$ cuts. The k^* distribution of these events is expected to be rather like that of true inner-bremsstrahlung $\pi\pi\gamma$ events. Further work is needed to completely resolve the inner-bremsstrahlung sample. In the fit shown in Figure 6 these events were assumed to have exactly the same k^* distribution as inner-bremsstrahlung events. Fits with various other assumptions were made, and it became evident that the effect of even the most extreme assumptions as to the shape and intensity of this background had no more than a 10% effect on the amount of direct emission given by the fits. This is because $k^* = \frac{M_{\pi\pi\gamma}^2 - M_{\pi\pi}^2}{2M_{\pi\pi\gamma}}$, and with a $\pi\pi$ mass resolution of ~ 4 MeV/c^2 it is nearly impossible for a $K^o_L \rightarrow \pi^+\pi^-$ induced background to affect the region with $k^* > 60$ MeV. The mean of the fits gives a branching ratio for $K^o_L \rightarrow \pi\pi\gamma$ of $\sim 5.5 \times 10^{-5}$. At the present stage of our analysis we attribute an error of $\pm 1.0 \times 10^{-5}$ to this figure, due mainly to uncertainties remaining in the normalization. The statistical error on any given fit is only $\sim \pm 0.4 \times 10^{-5}$. This number corresponds to about 300 directly emitted $\pi\pi\gamma$'s in the present sample. The one previous experiment yielding a positive result, found $\frac{K^o_L \rightarrow \pi^+\pi^-\gamma_{direct}}{K^o_L \rightarrow all} = 6.0 \pm 2.0 \times 10^{-5}$,[12] based on 24 events.

Figure 7 is a plot of $(1-\cos\theta_{ee\gamma}) \times 10^5$ vs $M(ee\gamma)$ for $ee\gamma$ candidates passing all other cuts. One event stands out as having an almost perfect mass and angle for a $K^o_L \rightarrow ee\gamma$ decay. When the usual cut on angle is made, no other event is closer than 100 MeV/c^2 from the K^o_L mass. This absence of any apparent background, and the fact that we know of no significant background process that contributes in this region leads us to accept the event as the first observed example of the decay $K^o_L \rightarrow ee\gamma$. The kinematic characteristics of the event are as follows $M_{ee\gamma} = 0.500$ GeV/c^2, $1-\cos\theta_{ee\gamma} = 0.015 \times 10^{-5}$ ((whereas $(1-\cos\theta_{ee}) = 0.497 \times 10^{-5}$)), $M_{ee} = 0.320$ GeV/c^2, $k^* = 0.147$ GeV/c. Although it may seem that the two-electron mass is rather high in view of the familiar low M_{ee} peaking in Dalitz decays, in fact our acceptance is so biased against low e-e mass events that the expected yield is rather flat in M_{ee}, all the way up to ~ 0.450 GeV/c^2. Accepting this event and calculating the acceptance assuming a Kroll-Wada type matrix element[5] leads to a branching ratio of $\frac{K^o_L \rightarrow e^+e^-\gamma}{K^o_L \rightarrow \text{all}} = 8.3 \pm 8.3 \times 10^{-6}$ which is certainly consistent with the prediction of a standard Kroll-Wada type calculation, 7.8×10^{-6}. Given this branching ratio we should see 4 - 5 events in our total sample.

There are no candidates for $K^o_L \rightarrow e^+e^-\pi^o$ events. Assuming that the number of events observed, (or unobserved) obeys Poisson statistics we quote an upper limit for the branching ratio corresponding to the observation of 2.3 events at the 90% confidence level. Calculating the acceptance with the assumption of a phase space distribution for the matrix element, we obtain an upper limit $\frac{K^o_L \rightarrow e^+e^-\pi^o}{K^o_L \rightarrow \text{all}} \leqslant 1.4 \times 10^{-5}$. We know of no previous experimental upper limit for this branching ratio. Potential $\mu^+\mu^-\gamma$ and $\mu^+\mu^-\pi^o$ decays are not separated as cleanly from background in our apparatus as are the corresponding electron decays. This is because the probability of accepting a pion as a μ is ~ 1 in 25, whereas the probability of accepting a pion as an e is < 1 in 10^5, and because the $\mu\mu\gamma$ and $\mu\mu\pi^o$ decays are kinematically much closer to $K^o_L \rightarrow \pi^+\pi^-\pi^o$ decays than are the $ee\gamma$ and $ee\pi^o$ modes. We find one event passing all cuts in both the case of $\mu\mu\gamma$ and of $\mu\mu\pi^o$. In each case this is consistent with our estimate of the background due to $K^o_L \to \pi^+\pi^-\pi^o$ so that we can claim no evidence for the observation of these decays. Again, quoting an upper limit corresponding to the observation of 2.3 events at the 90% c.l., we find $\frac{K^o_L \to \mu\mu\gamma}{K^o_L \to \text{all}} \leqslant 1.3 \times 10^{-6}$ where we have used a Kroll-Wada type matrix element in the Monte Carlo calculation of the $\mu\mu\gamma$ acceptance. This is approximately a 5-fold improvement in the previous upper limit.[13] The branching ratio predicted by the standard theory[5] is $\sim 2 \times 10^{-7}$. Proceeding in a similar manner for the $\mu\mu\pi^o$ case we find an upper limit of $\frac{K^o_L \to \mu^+\mu^-\pi^o}{K^o_L \to \text{all}} \leqslant 2.5 \times 10^{-6}$ at the 90% c.l. Here we have used a phase space distribution in the calculation of the acceptance. This represents a 20-fold reduction in the best previous upper limit for this decay.[13]

In summary, with 25% of our data sample analyzed, we have measured the branching ratio $\frac{K^o_L \to \pi^+\pi^-\gamma_{\text{direct}}}{K^o_L \to \text{all}}$, and have found the matrix element to be consistent with a CP-conserving M1 transition. We have observed the first example of the decay $K^o_L \to e^+e^-\gamma$ and have established improved upper limits for the branching ratios of the decays $K^o_L \to e^+e^-\pi^o$, $\mu^+\mu^-\gamma$, and $\mu^+\mu^-\pi^o$.

References

1. D. Beder, Nucl. Phys. B47, 286 (1972)

   A. Dolgov and L. Ponomarev, Soviet Journal of Nucl. Phys. 4,262 (1967).

   G. Coster and P.B. Kabir, Nuovo Cimento 51A, 564 (1967).

   L. Sehgal and L. Wolfenstein, Phys. Rev. 162, 1362 (1967).

2. M. Moshe and P. Singer, Phys. Rev. D6, 1379 (1972).

   R. Rockmore and T. Wong, Phys. Rev. D7, 3425 (1973).

   C.S. Lai and B.L. Young, Nuovo Cimento 52A, 7383 (1967).

   S.V. Pepper and Y.Ueda, Nuovo Cimento 33, 1614 (1964).

   S. Oneda, Y.S. Kim, D. Korff, Phys. Rev. 136, B1064 (1964).

   R. Rockmore, Phys. Rev. D1, 226 (1970).

   S. Barshay, Phys. Lett. 36B, 571 (1971).

3. S. Singh, Phys. Rev. D6, 2646 (1972).

   W. Alles and J. Pati, Nuovo Cimento 10A, 325 (1972).

4. L. Sehgel, Phys. Rev. D7, 3303 (1973).

5. T. Miyazaki, Nuovo Cimento Lett. 3, 294 (1972).

6. M.K. Gaillard and B.W. Lee, NAL-PUB-74/21-THY (1974).

   A. Pais and S. Treiman, Phys. Rev. 176, 1974 (1968).

   S. Singh and L. Wolfenstein, Nucl. Phys. B24, 77 (1970).

   S. Okubo and M. Bace, Nucl. Phys. B40, 541 (1972).

7. W.C. Carithers et al., Phys. Rev. Lett. 30, 1336 (1973).

8. T_i refer to elements of a 12 scintillation counter timing hodoscope placed just downstream of the Č counter. This hodoscope is designed so that each counter corresponds to one Č counter sector.

9. PO2 is a kinematic quantity which in the absence of errors is >0 for $K^o_L \to 3\pi$ decays, and almost always <0 for $K^o_L \to \pi\pi\gamma$ decays. For a definition and further discussion of the quantity see, e.g. D. Luers et al., Phys. Rev. 133, B1276 (1964).

10. Particle Data Group, Rev. Mod. Phys. 48, No. 2, pt. II (1976).

11. χ^2 = 6.6/12 degrees of freedom for a fit between k^* = 20 and 160 MeV.

12. G. Donaldson et al., Phys. Rev. Lett. 33, 554 (1974). We have renormalized their branching ratio to the current value of the $K^o_L \to \pi^+\pi^-\pi^o$ branching ratio.

13. G. Donaldson, Ph. D. thesis, SLAC-184 (unpublished).

Figure Captions

1. Layout of the apparatus.

2. $M(\gamma\gamma)$ for a sample of $\pi^+\pi^-\gamma\gamma$ events

3. $M(\pi^+\pi^-\gamma\gamma)$ for events in which $.105 < M(\gamma\gamma) < .165$ GeV/c^2

4. $M(\pi^+\pi^-\gamma)$ for a sample of $\pi\pi\gamma$ candidates with $(1-\cos\theta_{\pi\pi\gamma}) < 0.3 \times 10^{-5}$.

5. $(1-\cos\theta_{\pi\gamma\gamma})\times 10^5$ for a sample of $\pi\pi\gamma$ candidates with $.48 < M_{\pi\pi\gamma} < .52$ GeV/c^2.

6. k^* distribution for all events passing the $\pi\pi\gamma$ cuts. A fit to inner bremsstrahlung + an M1 direct transition is shown.

7. $(1-\cos\theta_{ee\gamma}) \times 10^5$ vs $M(ee\gamma)$ for $ee\gamma$ candidates passing all other cuts.

FIGURE 1

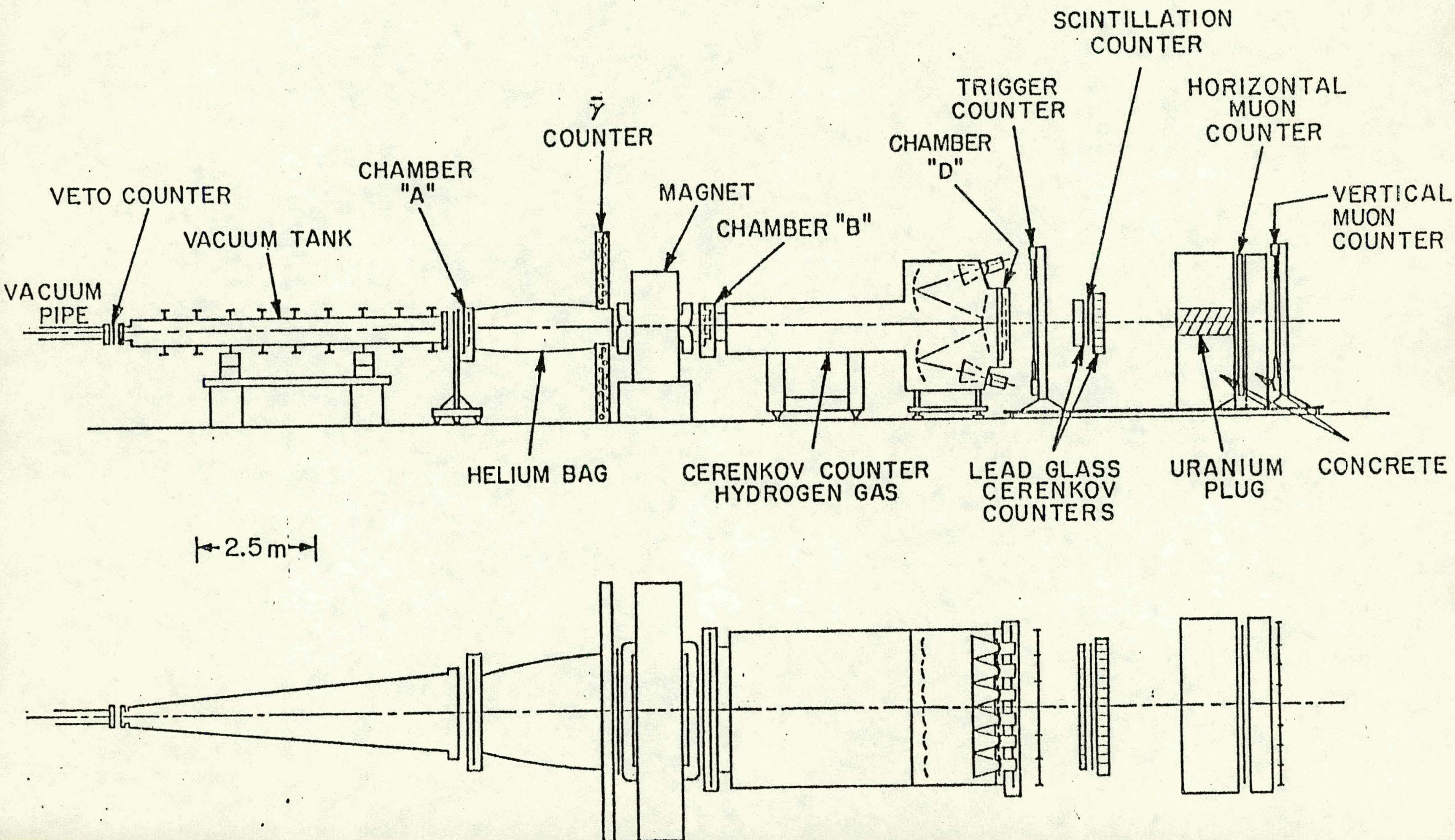

SCINTILLATION COUNTER
TRIGGER COUNTER
HORIZONTAL MUON COUNTER
$\bar{\gamma}$ COUNTER
CHAMBER "D"
CHAMBER "A"
MAGNET
VERTICAL MUON COUNTER
VETO COUNTER
CHAMBER "B"
VACUUM TANK
VACUUM PIPE
HELIUM BAG
CERENKOV COUNTER HYDROGEN GAS
LEAD GLASS CERENKOV COUNTERS
URANIUM PLUG
CONCRETE
2.5 m

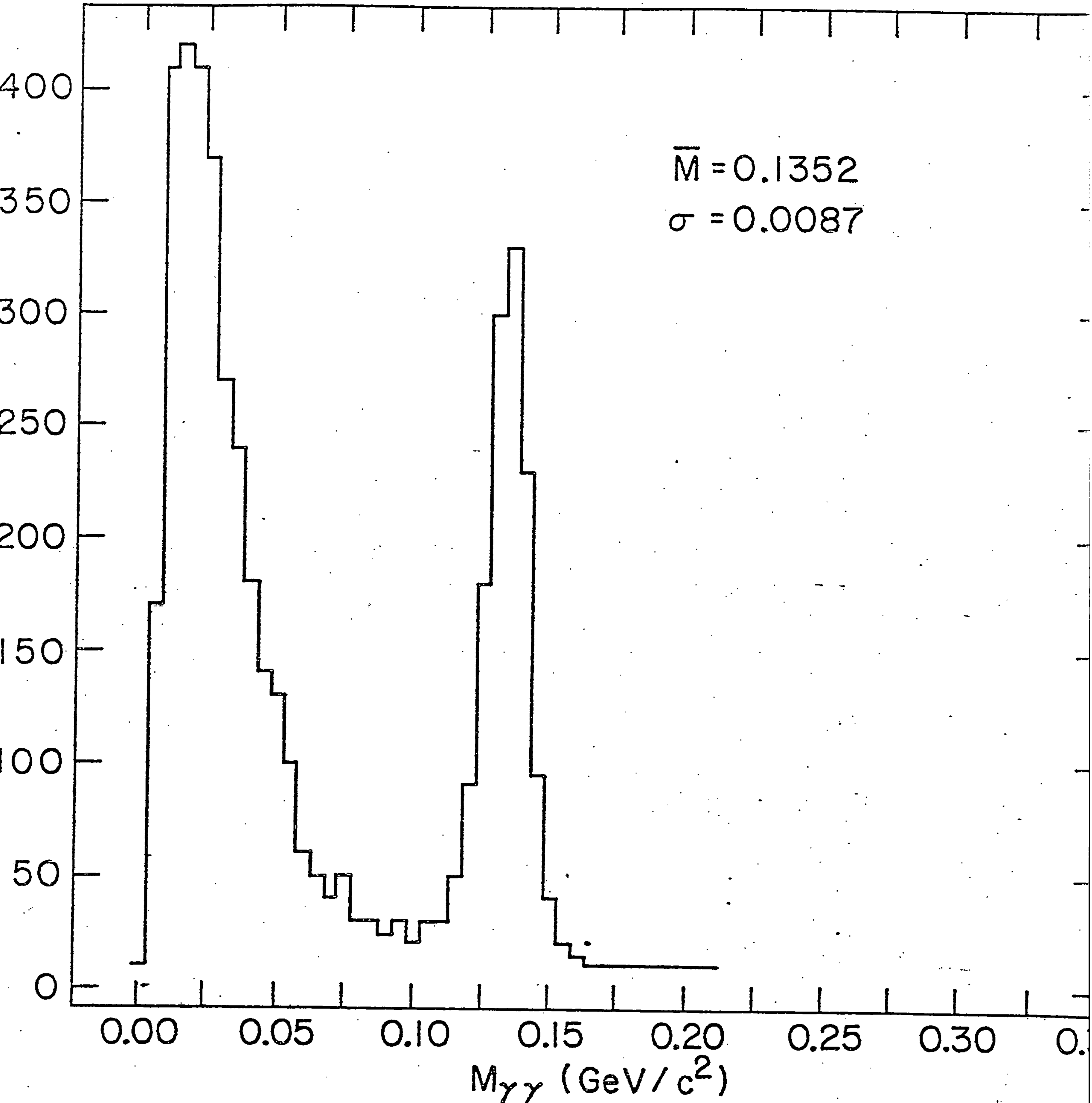

400
350
300
250
200
150
100
50
0
$\overline{M}$ = 0.1352
σ = 0.0087
0.00
0.05
0.10
0.15
0.20
0.25
0.30
$M_{\gamma\gamma}$ (GeV/c^2)

FIGURE 2

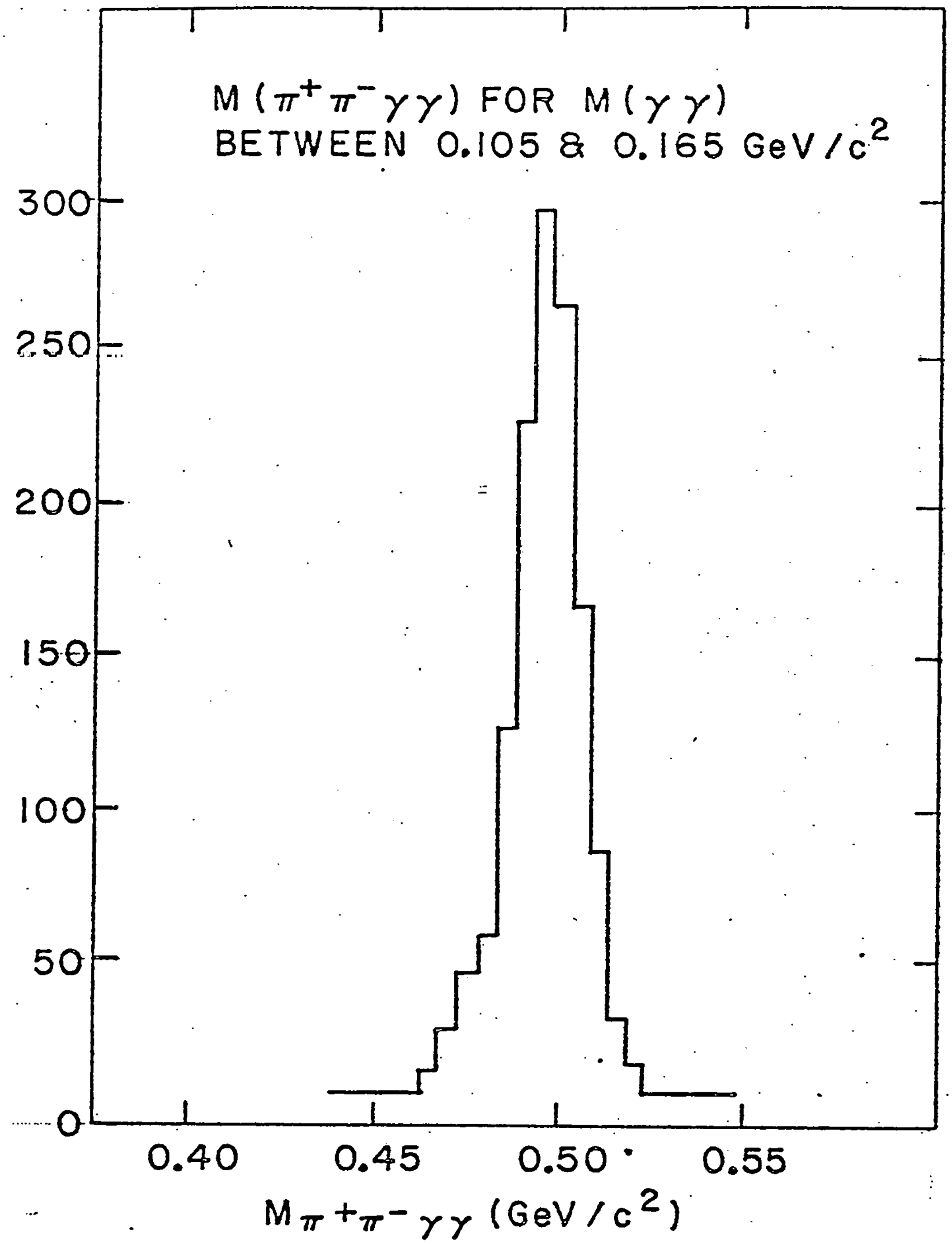
M ($\pi^+\pi^-\gamma\gamma$) FOR M ($\gamma\gamma$)
BETWEEN 0.105 & 0.165 GeV/c^2
300
250
200
150
100
50
0
0.40
0.45
0.50
0.55
$M_{\pi^+\pi^-\gamma\gamma}$ (GeV/c^2)

FIGURE 3

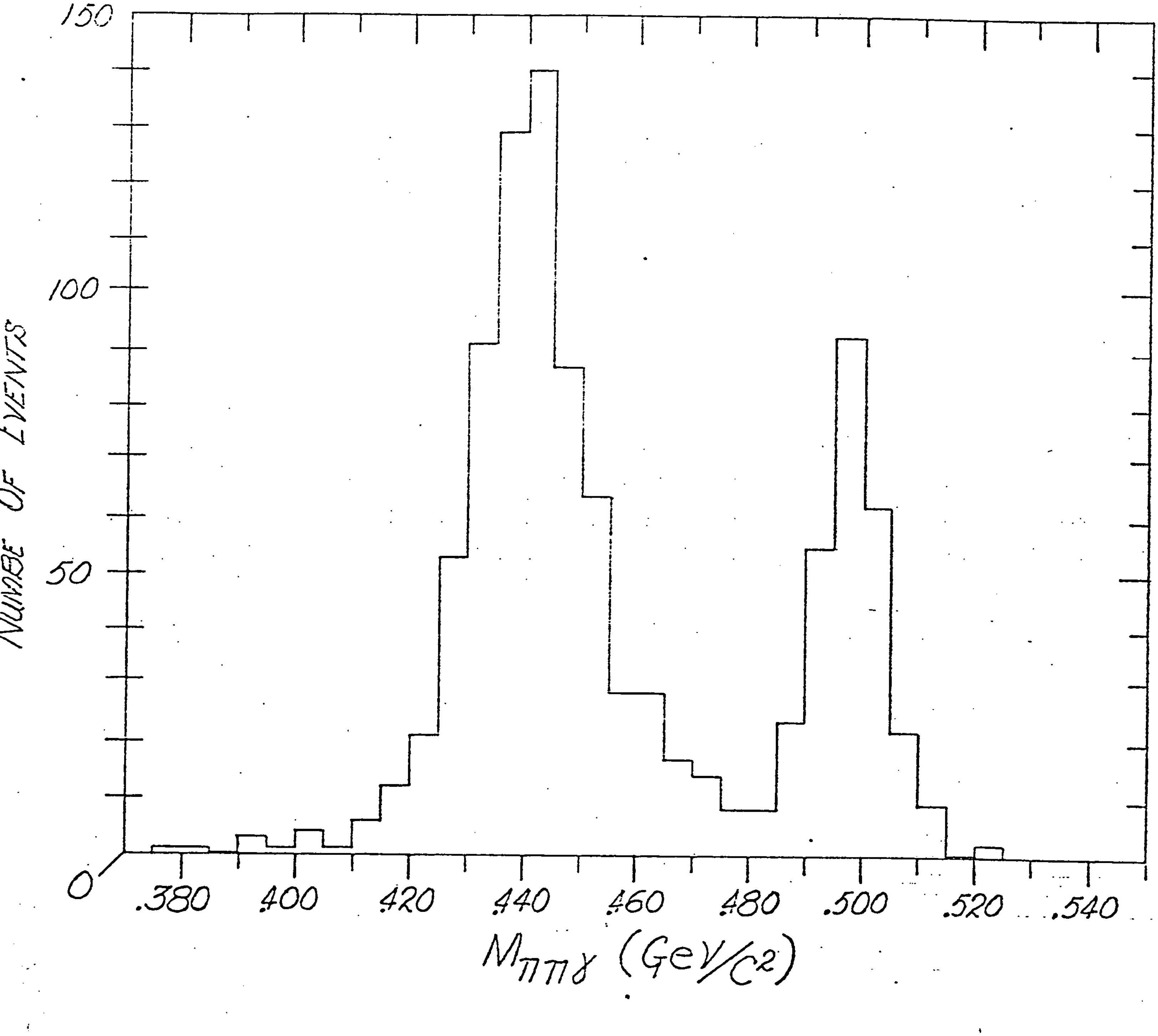

150
100
50
0
NUMBE OF EVENTS
.380
.400
.420
.440
.460
.480
.500
.520
.540
$M_{\pi\pi\gamma}$ (GeV/C²)

FIGURE 4

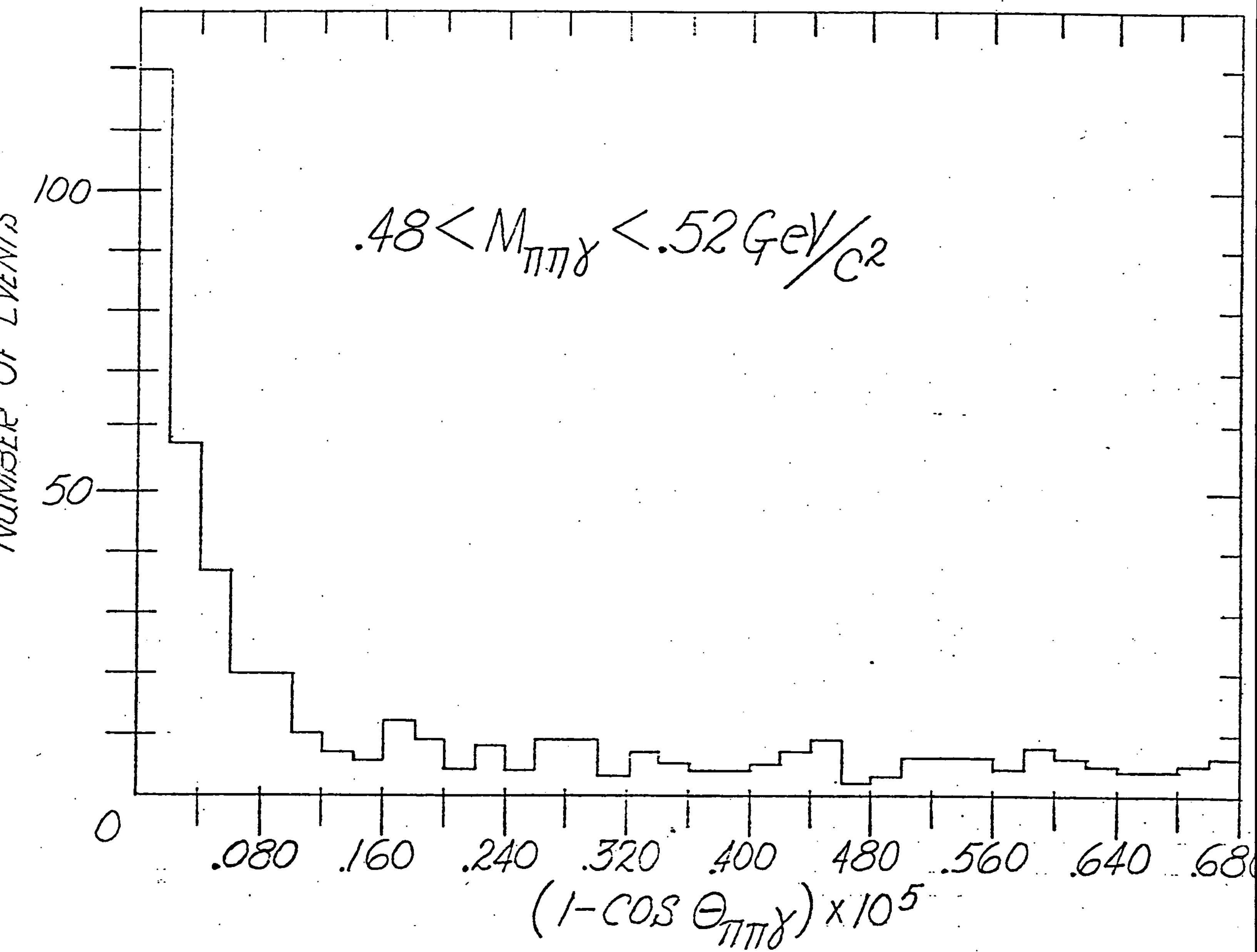

NUMBER OF EVENTS
100
50
0
.48 < M ππγ < .52 GeV/c²
.080 .160 .240 .320 .400 480 .560 .640 .680
(1-COS Θ ππγ) x 10⁵

FIGURE 5

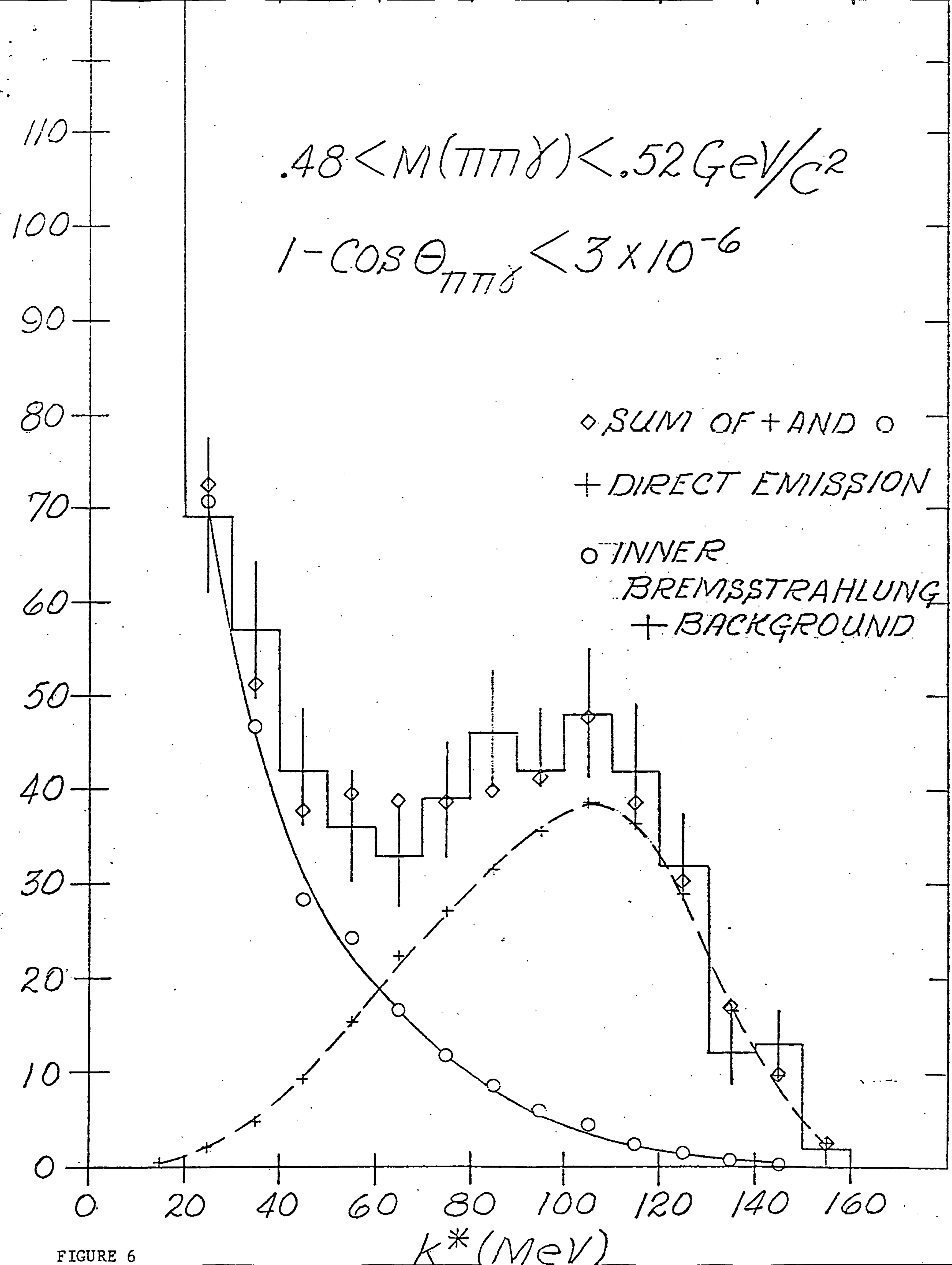

.48 < M(ππγ) < .52 GeV/c²
1 - Cos θππγ < 3 x 10⁻⁶
◇ SUM OF + AND ○
+ DIRECT EMISSION
○ INNER BREMSSTRAHLUNG + BACKGROUND
0
10
20
30
40
50
60
70
80
90
100
110
0
20
40
60
80
100
120
140
160
k*(MeV)

FIGURE 6

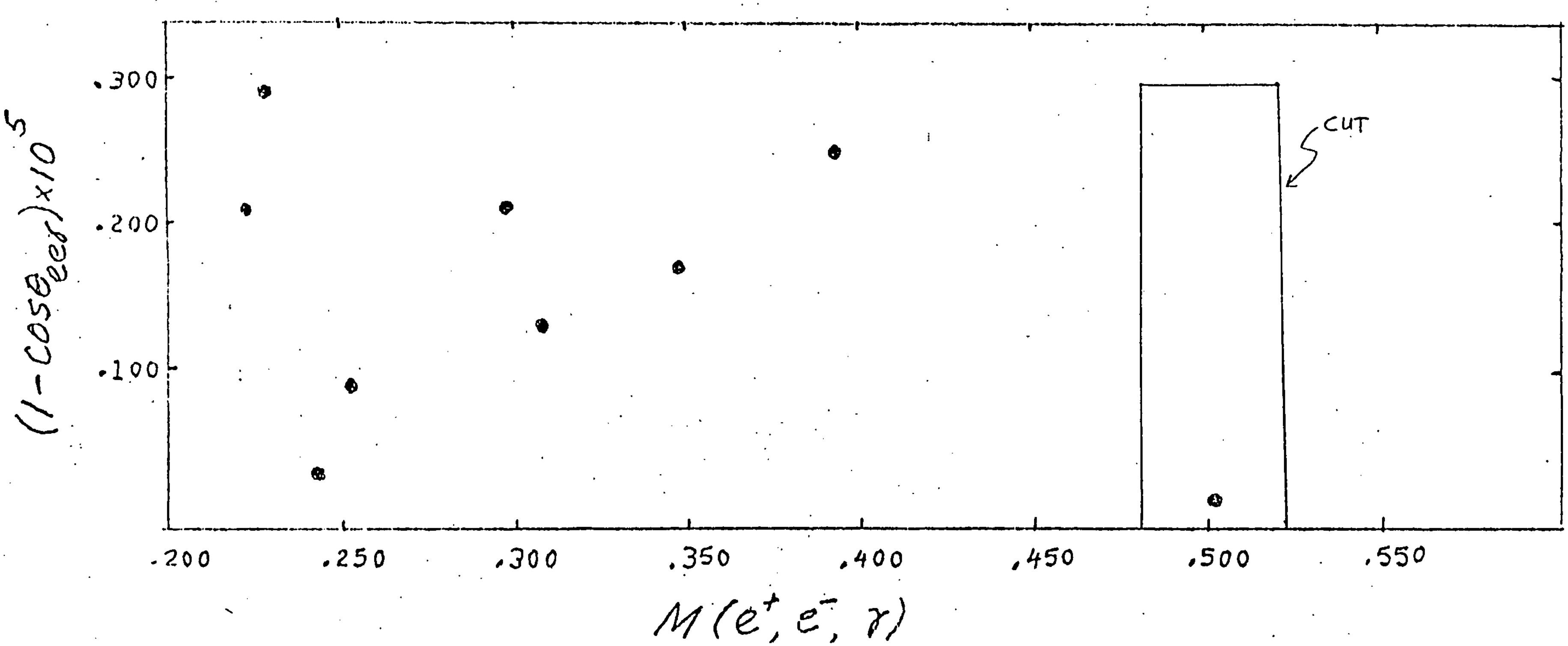

.300
.200
.100
$(1-\cos\theta_{ee\gamma})\times 10^5$
CUT
.200
.250
.300
.350
.400
.450
.500
.550
$M(e^+, e^-, \gamma)$

FIGURE 7